A 21-Event, 4,000-Year History of Surface Ruptures in the Anza Seismic Gap, San Jacinto Fault, and Implications for Long-term Earthquake Production on a Major Plate Boundary Fault

Thomas K. Rockwell, Timothy E. Dawson, Jeri Young Ben-Horin & Gordon Seitz

Pure and Applied Geophysics
pageoph

ISSN 0033-4553

Pure Appl. Geophys.
DOI 10.1007/s00024-014-0955-z

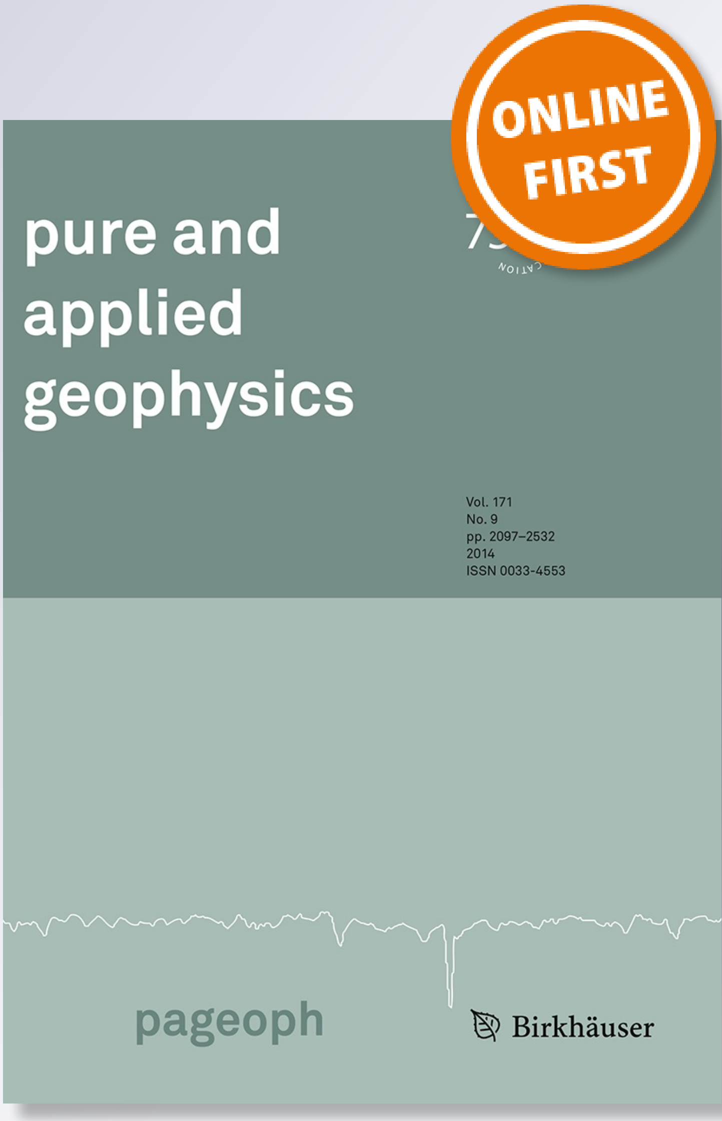

Pure Appl. Geophys.

DOI 10.1007/s00024-014-0955-z

Pure and Applied Geophysics

A 21-Event, 4,000-Year History of Surface Ruptures in the Anza Seismic Gap, San Jacinto Fault, and Implications for Long-term Earthquake Production on a Major Plate Boundary Fault

Thomas K. Rockwell,[1] Timothy E. Dawson,[2] Jeri Young Ben-Horin,[3] and Gordon Seitz[2]

Abstract—Paleoseismic work completed at Hog Lake on the San Jacinto Fault (SJF) near Anza, California, indicates that at least 21 surface ruptures have occurred in the Anza Seismic gap over the past 4,000 years. The ages of the ruptures are constrained by 111 radiocarbon dates, 97 of which fall in stratigraphic order. The average recurrence interval for all ruptures for this period is about 185 ± 105 years, although some ruptures, such as occurred in the April 1918 earthquake, caused only minor displacement. We rate the expression of each interpreted event in each of the twelve developed field exposures presented in this work by assigning numeric values for the presence of different criteria that indicate rupture to a paleo-ground surface. Weakly expressed ruptures, for example the deformation we interpret to be the result of the historical 1918 earthquake, received low scores and are interpreted as smaller earthquakes. From this analysis, we infer that at least fifteen of the identified ruptures are indicative of large earthquakes similar to the penultimate earthquake, inferred to be the M_w 7.3 22 November 1800 earthquake. The adjusted recurrence interval for large earthquakes lengthens to approximately 254 years. Comparison with the rupture history at the Mystic Lake paleoseismic site on the Claremont strand indicates that it is plausible that several of the large ruptures identified at Hog Lake could have jumped the Hemet step-over at Mystic Lake and continued on the Claremont strand (or vice versa), but most of the event ages do not match between the two sites, indicating that most ruptures do not jump the step. Finally, comparison with San Andreas Fault ruptures both to the north and south of its juncture with the SJF suggest that some northern SJF ruptures identified at Mystic Lake may correlate with events identified at Wrightwood, but that these northern ruptures have no match at Hog Lake and can not indicate rupture of the entire SJF onto the SAF.

Key words: Paleoseismology, San Jacinto fault, Earthquake recurrence patterns, Fault behavior.

Electronic supplementary material The online version of this article (doi:10.1007/s00024-014-0955-z) contains supplementary material, which is available to authorized users.

[1] Geological Sciences, San Diego State University, San Diego, CA 92182, USA. E-mail: trockwell@mail.sdsu.edu

[2] California Geological Survey, Menlo Park, CA 94025, USA.

[3] Arizona Geological Survey, 416 W. Congress, Suite 100, Tucson, AZ 85701, USA.

1. Introduction

Long records of past earthquakes on major plate boundary faults reveal the long-term temporal and spatial patterns of moderate to large earthquake production, thus providing a means of testing whether earthquake behavior is periodic, random, or clustered in time. Moreover, long records provide a means of forecasting the likely occurrence of future large earthquakes on that fault. Development of a long rupture record requires both excellent stratigraphy and the ability to date numerous stratigraphic layers with relatively high precision, conditions that exist at a relatively few investigated sites (Sieh 1978; Scharer *et al.* 2007, 2010; Fumal *et al.* 2002; Lienkaemper and Williams 2007; Lienkaemper *et al.* 2010; Berryman 2012). Most paleoseismic sites are limited to the dating of just the past few surface ruptures (Lindvall 2002; Grant and Sieh 1994; Stone *et al*. 2002; Young *et al*. 2002), whereas some have records that extend back to a dozen or fewer events. The longest record has been developed at the Wrightwood paleoseismic site along the San Andreas Fault, where as many as 30 events have been recorded over the past 5,000 years, although the middle part of the record is incomplete (Fumal *et al.* 2002; Scharer *et al.* 2007, 2010).

In this paper, we present evidence of as many as 21 surface ruptures over the past 4,000 years that have been recorded in the stratigraphy at Hog Lake, a sag pond along the central San Jacinto Fault near Anza, California (Figs. 1, 2). Hog Lake is an ephemeral pond with centimeter-scale stratigraphic resolution and numerous peat-like organic layers indicative of periods of non-deposition punctuated by brief periods of clastic deposition. Most of the peat-

Birkhäuser

Journal : Small 24 | Dispatch : 28-10-2014 | Pages : 23
Article No. : 955 | LE | TYPESET
MS Code : PAAG-1383 | CP | DISK

Figure 1
Faults and referenced paleoseismic sites mentioned in the text (*hexagons*) along the southern San Andreas Fault system in southern California. Also note the locations of Spanish missions (*stars*) that reported (or did not report) the earthquake in November, 1800. *SB* Santa Barbara, *V* Ventura, *SF* San Fernando, *SG* San Gabriel, *LA* Los Angeles, *SJC* San Juan Capistrano, *SD* San Diego

like layers contain small seeds, and most stratigraphic units contain charcoal, providing the ability to develop a precise chronology of sedimentation, and thus earthquake ages. The San Jacinto Fault bisects the pond, providing the opportunity to study the interaction between surface ruptures and sedimentation, making it an ideal paleoseismic environment. Using this long record, we investigated the variability in earthquake production for the central San Jacinto Fault, and compared its earthquake history to that of a site at Mystic Lake, located about 47 km farther north along the Claremont strand of the fault zone. We also compared these results with the rupture history recorded at sites along the San Andreas Fault and discuss plausible scenarios of fault interaction.

2. *Structural Setting of Hog Lake*

The San Jacinto Fault is a major structural element of the southern San Andreas Fault system in southern California. The Clark strand is the primary strand of the central San Jacinto Fault zone. Sharp (1967) suggested a total offset of ~25 km based primarily on the offset of the Thomas Mountain Sill, with most of that total on the Clark strand itself (Fig. 2a). Thus, slip rates on the central Clark strand should be a good representation of the slip rate of the San Jacinto Fault. Some workers have suggested that the San Jacinto Fault and San Andreas Fault may accommodate subequal amounts of the current plate boundary slip (Bennett *et al*. 2004; Fialko 2006; Blisniuk *et al*. 2010). The late Quaternary slip rate of the Clark strand (Fig. 2b) has been estimated to be approximately 12–14 mm/year at Anza (Rockwell *et al*. 1990; Blisniuk *et al*. 2013). The Holocene rate at Anza was estimated to be about 15 ±3 mm/year for the past 4,300 years based on the offset of a beheaded buried channel dated by ^{14}C (Merifield *et al*. 1991). These rates are comparable with or slightly lower than geodetic rates (Bennett *et al*. 2004). Recent work to the south indicates that the slip rate drops towards the

Journal : Small 24 | Dispatch : 28-10-2014 | Pages : 23
Article No. : 955 | ☐ LE | ☐ TYPESET
MS Code : PAAG-1383 | ☑ CP | ☑ DISK

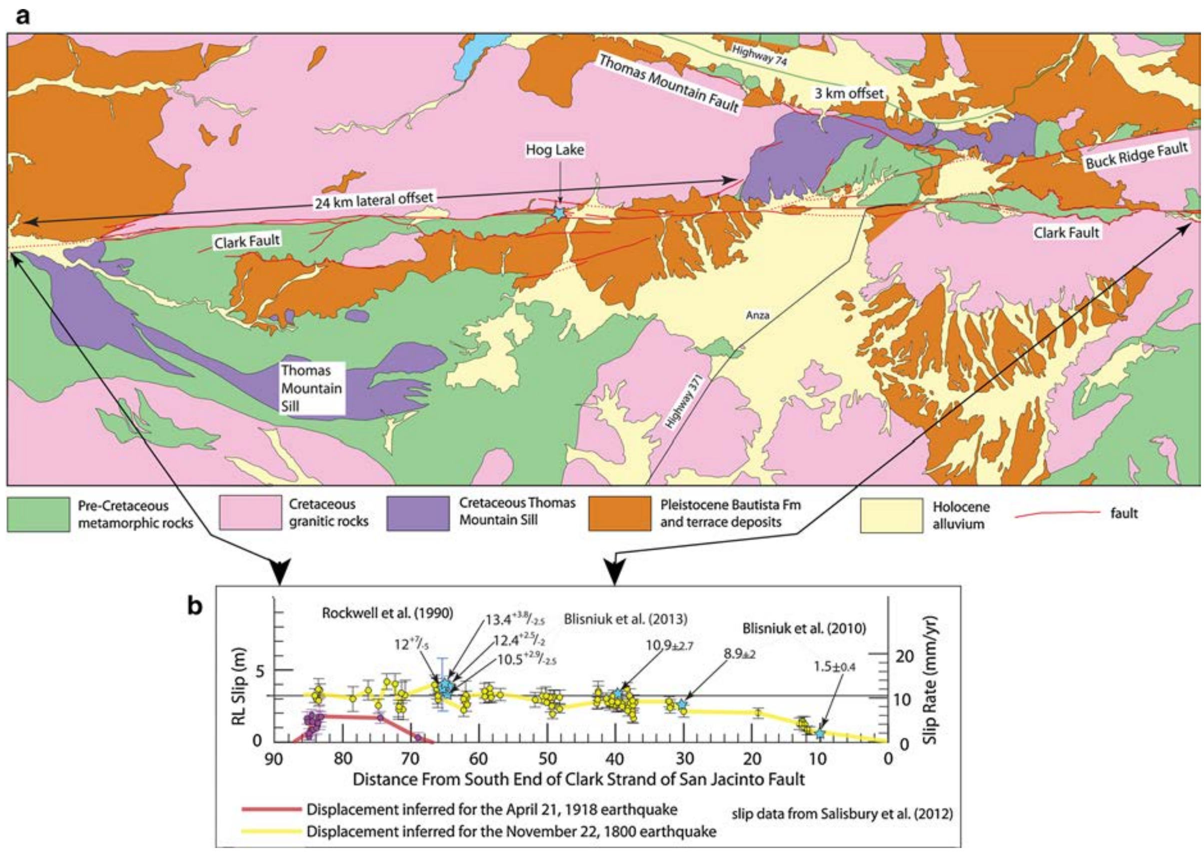

Figure 2

a Geological map of the south-central San Jacinto fault showing the offset of the Thomas Mountain Sill, the location of Hog Lake, and secondary faults. Geology simplified from Sharp (1967). **b** Slip distribution for the two most recent Clark fault ruptures, inferred to have resulted from the 1918 and 1800 earthquakes (Salisbury *et al.* 2012) plotted with slip rate estimates and uncertainties (Rockwell *et al.* 1990; Blisniuk *et al.* 2010, 2013) suggesting that slip rate is built by repeated ruptures similar to these historical earthquakes

southern end of the Clark Fault, presumably as slip is transferred to the Coyote Creek and Buck Ridge strands southeast of Anza (Blisniuk *et al.* 2010) (Fig. 2b). Comparison of slip distribution inferred for the most recent event (Salisbury *et al.* 2012) with the many slip rate determinations along the Clark fault suggests that slip rate is built by repeated large displacements on the fault, as recorded in the young geomorphology (Fig. 2b). Ideally, earthquake production over the past several thousand years, as recorded at Hog Lake, should also be sufficient to accommodate the long-term slip rate, so the 4,000 year earthquake record at Hog Lake should be a reasonable representation of the long-term production rate along the central San Jacinto Fault.

Hog Lake lies within the Anza seismic gap of Sanders and Kanamori (1984) (Fig. 3), which has been interpreted as a locked or high-strength section of the central San Jacinto Fault; seismicity reaches as deep as 20 km on either side of the gap. Slip distributions have been determined for the past three surface ruptures along the Clark Fault through the seismic gap from such offset geomorphic features as rills, small channels, and alluvial bars (Salisbury *et al.* 2012). Displacement through the Anza area is estimated to have reached a maximum of 3–4 m for each of the past three large prehistoric events, with rupture from the moderate M_w 6.9 1918 earthquake extending northwest of the gap from Hog Lake to Hemet (Salisbury *et al.* 2012) (Fig. 2b). Displacement from the three larger earthquakes is interpreted to decrease to the southeast of Anza and to the northwest of Hog Lake, which supports the idea that the seismicity gap is the strongest structural element

Journal : Small 24 | Dispatch : 28-10-2014 | Pages : 23
Article No. : 955 | LE | TYPESET
MS Code : PAAG-1383 | CP | DISK

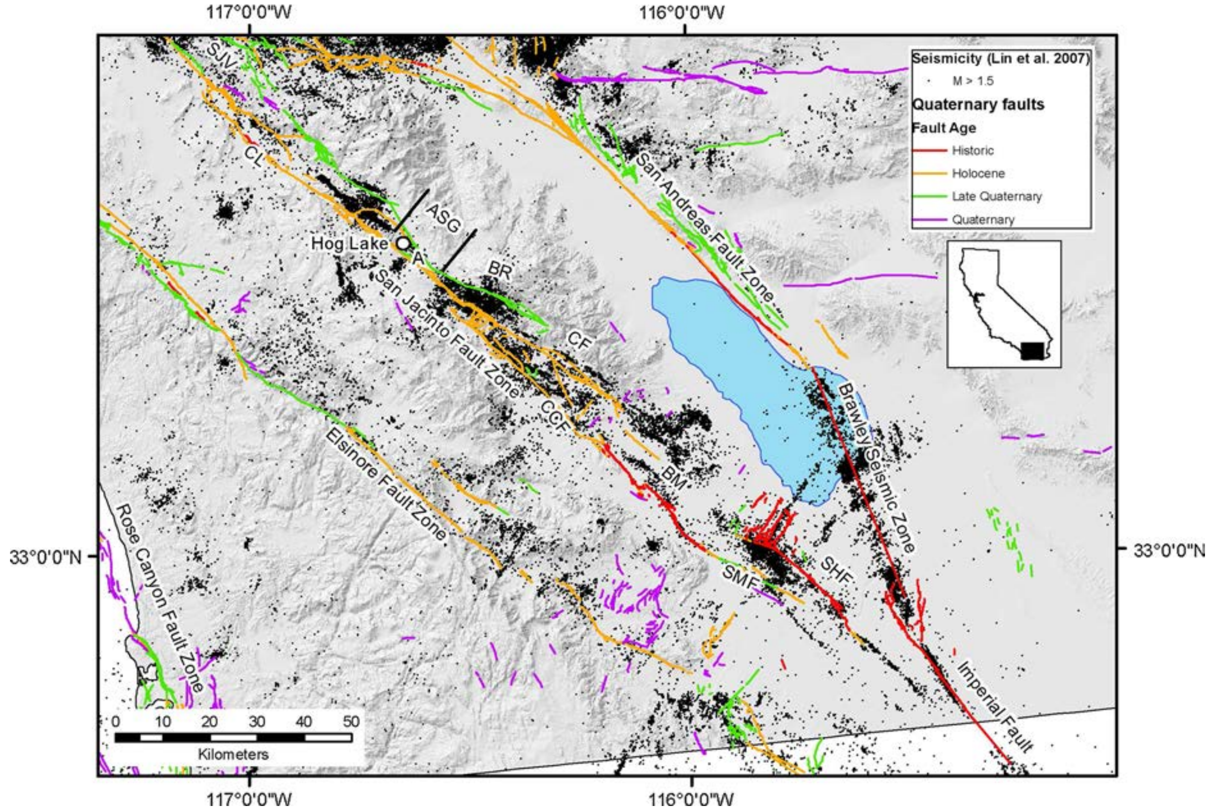

Figure 3
Seismicity (*black dots*) along the San Jacinto fault (from Lin *et al.* 2007). Historical ruptures are denoted in *red*, Holocene faults in *orange*, late Quaternary faults in *green*. Note the abundant seismicity southeast of Anza where the fault zone splays into the Buck Ridge (*BR*), Clark (*CF*), and Coyote Creek (*CCF*) faults. Also shown are the Claremont Fault (*CL*), Superstition Hills Fault (*SHF*), and Superstition Mountain Fault (*SMF*). Many small northeast-striking cross faults are present between these major strands, several of which have produced moderate (M_w 4.8–5.9) earthquakes in recent decades (1937, 2001, 2005, 2009, 2012). In the Anza area northward to Hog Lake, seismicity is suppressed, leading Sanders and Kanamori (1984) to name this section the Anza Seismicity Gap (*ASG*)

of the central San Jacinto Fault zone, assuming each 3–4 m displacement represents the maximum displacement of a single earthquake.

Hog Lake occupies a small releasing step in the fault between two major alluvial fans that drain large catchments along the southwest flank of Thomas Mountain (Fig. 4). The two alluvial fans presumably supply most or all of the sediment to the Hog Lake depression. Of note is the fact that the large alluvial fan to the south of Hog Lake is the drainage divide between the Hemet and Santa Margarita regional catchment systems; Hog Lake drains northwestward into the Hemet basin catchment system. The smaller, northern alluvial fan acts as a block to this northwesterly flow, resulting in an additional control for the closed depression. The releasing step-over is of the order of 100 m in width, smaller than Hog Lake itself, so this blockage is probably more important than the small structural step in the formation of Hog Lake. During wet years, water is supplied from both areas of drainage, but the southern drainage has a much larger catchment area and is likely to supply most of the water and sediment. Flow to the north is achieved once the pond fills to a depth of approximately 1.5 m, the spillway height around the toe of the northern fan. As the locus of fine-grained sedimentation seems to have been somewhat stationary, it seems that there is a dynamic balance between aggradation of the fan and sedimentation within the pond, providing the necessary characteristics to preserve a long record of fine-grained stratigraphy.

Journal : Small 24 | Dispatch : 28-10-2014 | Pages : 23
Article No. : 955 | ☐ LE | ☐ TYPESET
MS Code : PAAG-1383 | ☑ CP | ☑ DISK

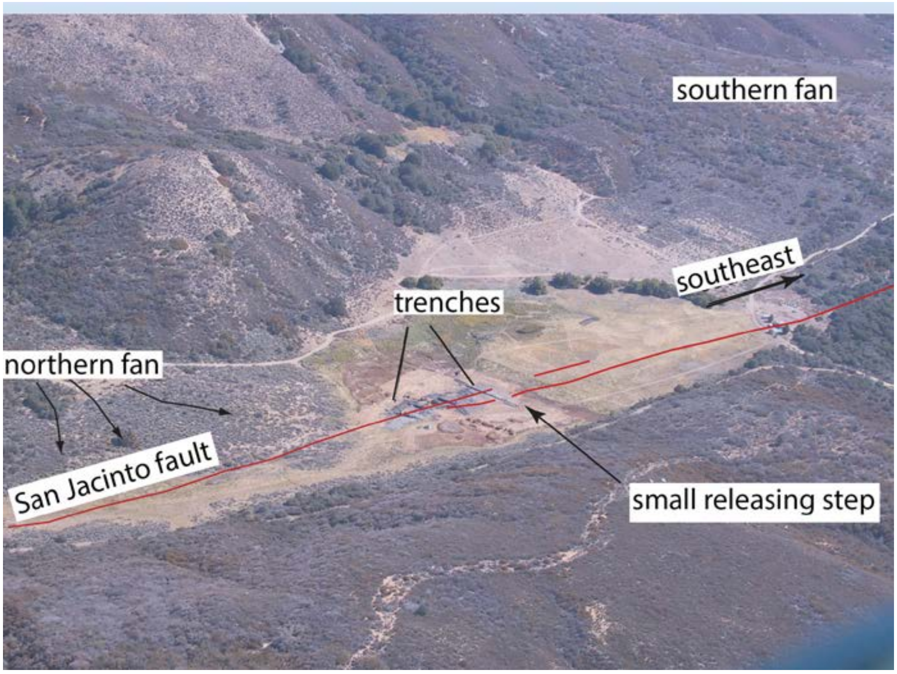

Figure 4
Oblique aerial photograph of the Hog Lake site with the base of Thomas Mountain toward the *upper left*. Note the large alluvial fan to the south that probably provides most of the water, and the smaller alluvial fan to the north that partially blocks the outflow and enables the formation of the shallow pond during the wet season

3. Site Stratigraphy

The trenches (Fig. 5) exposed excellent stratigraphy at Hog Lake, with the resolution of strata improving toward the deepest parts of the depression (full-resolution logs are given in the electronic supplement). The sediments range in particle size from clay to gravel, with most in the sandy silt to silt particle class. Organic accumulations separate many of the strata, with the amount of organics varying across different areas of the depression. In some cases, a dense, centimeter-thick peat-like accumulation of organics is probably indicative of burial of an organic mat during a large storm. Such a layer can be seen to thin, disappear, or merge into an organically-enriched, darkened soil (A horizon) toward the pond margins. We interpret the organic layers as periods of non-deposition and soil formation, or, for the wettest and/or lowest areas of the depression, organic accumulation. The sediment layers, in contrast, are interpreted as representing punctuated storms during which sediment was transported from the watershed to the basin. The uppermost strata are capped by a thick A horizon soil, which indicates that the site is substantially drier now than for most of its past 4,000-year history.

We differentiated units on the basis of their lateral continuity, grain size distribution, color, and the presence or absence of separating organic layers. In many cases it was clear that an organic layer at the top of some units was related to soil-formation processes, but because the organic layers were very important in the lateral correlation of strata and packages of strata, most of the organic layers are given individual unit designations.

Some of the organic units merge laterally with strongly oxidized, bright orange sediments that we interpret as surface burn layers. Some of these burn layers are present in all exposures and probably represent complete burning of the site. For other such strata, the burning was apparently limited to the dry sections of the depression, as oxidized layers west of the fault, where the surface is relatively uplifted and water-free during the dry season, changed to unburned organic-rich peat-like strata in the deeper parts of the depression east of

Journal : Small 24 | Dispatch : 28-10-2014 | Pages : 23
Article No. : 955 | ☐ LE | ☐ TYPESET
MS Code : PAAG-1383 | ☑ CP | ☑ DISK

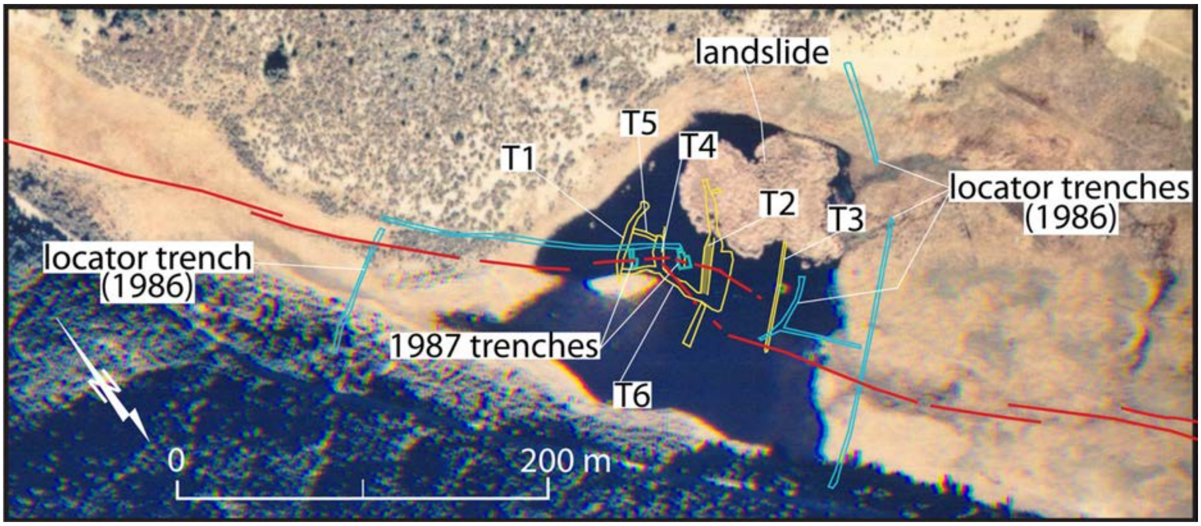

Figure 5
Map of trenches excavated at Hog Lake over four field seasons. Preliminary fault-location trenches across the entire valley enabled the locations of the main and secondary fault strands to be established. Subsequent work focused on the interaction of repeated faulting and sedimentation in the pond to establish the record of past surface ruptures

the fault which were, presumably, wet at the time of burning.

The units are numbered from top to bottom, with increasing numbers downward with increasing age, as we excavated deeper trenches during the latter part of the investigation (full-resolution logs are given in the electronic supplement). We primarily numbered the major units that could be traced from trench to trench, and excavated fault-parallel trenches for stratigraphic correlation so that all common strata share a common unit designation. In some areas of the depression, units splayed into multiple discrete stratums; this was particularly evident toward the primary depo-center near trench T2 (Fig. 5). As we initially named the units in our first trench, T1, this required subdividing the units into multiple sub-units and designating them with a lower-case letter, for example 149a, 149b, and 149c. We did this where designation of discrete strata was important in interpretation of faulting events. In other cases, there are more discrete units defined for some trench logs, although we did not assign a unit name to every recognizable stratum. We also did not name some units for which the correlation was uncertain or speculative.

We used the organic soil layers as primary correlation features, because they are interpreted as representing the years or decades between large storms, and because they were found to be laterally continuous in most or all exposures. As many of these were partially or completely burned, producing the oxidized horizons, these particular layers were useful in correlating strata for which the fault-parallel trenches were not deep enough to trace all of the older strata directly on the trench faces.

Most of the sediments in Hog Lake are very fine sand to silt in size, or finer, but several major sand (and locally gravel) units indicative of a few distinct flooding events account for a significant volume of the sediment (discussed in the stratigraphic section in the electronic supplement). We interpret the sand and gravel packages of units 150, 225, 550, 590–605, and 750 as indicative of major storms that caused significant erosion and transport in the catchment areas of the two fans, resulting in deposition of coarse strata in the Hog Lake depression. The distinctive sand of unit 150 in trench T1 is clearly derived from the northern fan as the sand pinches out southward. Similarly, the coarse sand and gravel of unit 225 both thins and becomes finer southward from the northern fan, indicating a northern fan source. The silt and clay are likely to have been derived from both sources and are aerially extensive throughout the pond.

Journal : Small 24	Dispatch : 28-10-2014	Pages : 23
Article No. : 955	□ LE	□ TYPESET
MS Code : PAAG-1383	☑ CP	☑ DISK

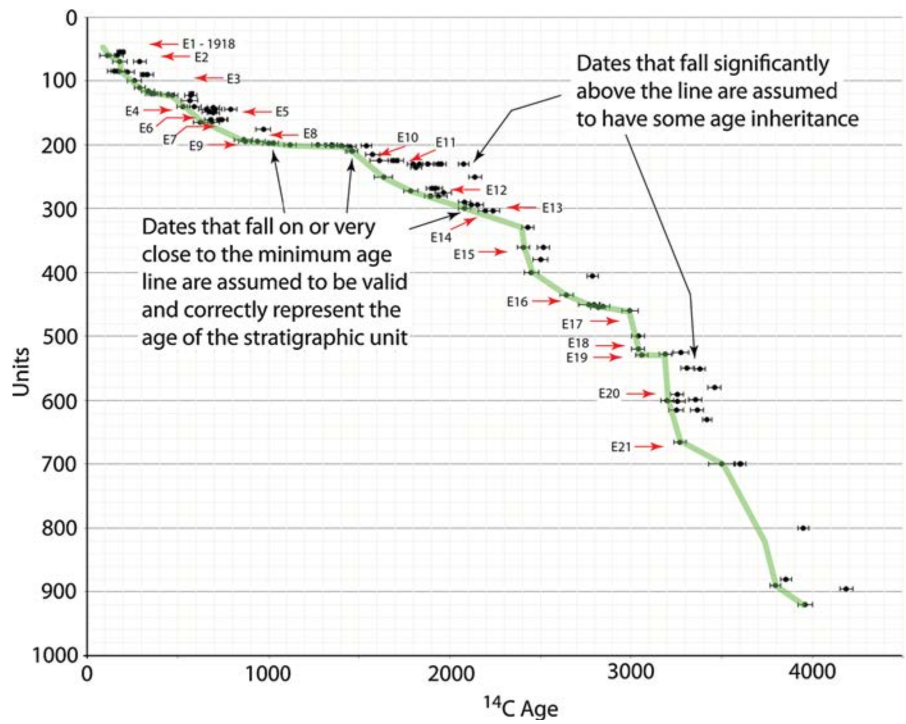

Figure 6
Radiocarbon ages versus depth, as determined by stratigraphic position, plotted with the stratigraphic locations of the 21 inferred event horizons. Note that most dates appear in stratigraphic order. The few that fall significantly above the line are assumed to have some inheritance. In model 1, we used the 97 dates that enable OxCal to complete its calculations. In model 2, we only used the dates that fall along the age/depth curve

4. *Age Control*

The stratigraphy at Hog Lake contained abundant seeds, carbonized or burned reeds, detrital charcoal, wood, root mats, and gastropod shells, all of which are potentially excellent samples for radiocarbon dating. We chose ~120 samples from the different trench exposures at Hog Lake for dating, and dated several different materials from several discrete layers to test the utility of all potential dating materials. The gastropod shells tended to yield older ages than the seeds, reeds, and most of the charcoal, suggesting a reservoir inheritance effect of older carbon. Because we did not date a sufficient number of shells to establish a good reservoir correction, and because reliable material for dating was abundant, we did not include the shell dates in our analysis. In contrast, nearly all dating of seeds yielded ages in correct stratigraphic order, suggesting relatively high reliability and lack of post-burial vertical motion or reworking. In total, we dated 111 samples of seeds, reeds, and charcoal to provide age control for the Hog Lake ruptures (the samples and their ages are listed in Table S1 in the electronic supplement).

The uncalibrated radiocarbon dates ranged in age from approximately 110 to 4,000 years, with increasing radiometric age corresponding to increasing stratigraphic depth (Fig. 6). A few dates were clearly out of stratigraphic order compared with those above and below, because they seem too old (Fig. 6). Consequently, we did not use these in our initial chronologic models.

We developed two chronological OxCal models (Bronk Ramsey *et al*. 2012) with which to date the paleo-earthquakes. In model 1 (electronic supplement, Part A), we used the 97 dates that do not violate stratigraphic ordering and placed them in their stratigraphic order in OxCal to provide dendrochronologically-corrected ages of individual stratums and the inferred paleo-surface ruptures. For this model, we used all dates that enabled OxCal to complete its calculations. In model 2, we excluded

Journal : Small 24 | Dispatch : 28-10-2014 | Pages : 23
Article No. : 955 | ☐ LE | ☐ TYPESET
MS Code : PAAG-1383 | ☑ CP | ☑ DISK

dates that we regarded as marginal because most of their probability distribution lay outside the overlying and underlying calibrated age distribution. For model 2, 85 dates were used to constrain the ages of strata and past surface ruptures. Both OxCal models, with the table of all radiocarbon dates, are supplied in the electronic supplement. However, in brief, removal of the marginal dates had little effect on the overall chronology of the Hog Lake sediments and tended to shift only a few of the event ages by a few decades. From these observations, we consider the overall chronology of the site to be well resolved within the stated uncertainties given below. Consequently, we report model 2 ages only in the next section when we discuss the ages of interpreted earthquakes.

5. Recognition and Timing of Earthquakes

Several criteria were used to identify evidence of past surface ruptures at Hog Lake. Specific evidence included the presence of filled fissure and major fault splays capped by unbroken strata, folding of strata with associated angular unconformities, the presence of buried scarps and growth strata on the down-thrown side of the fault, or where folding occurred on the western up-thrown side, growth strata west of the main fault, and the presence of flame structures, sand blows, or other evidence of rapid dewatering and liquefaction (Weldon *et al*. 1996; McCalpin *et al*. 2009). Because any one exposure is unlikely to express all of these phenomena for every rupture, it was critical to establish continuity of stratigraphic units that are coherent throughout the site to demonstrate that fault-related features are coeval. Where the oldest strata were exposed, in trenches T4 and T2, the deepest strata were correlated by the unique sequence of stratigraphic layers that included thick sand horizons (unit 750) and burn horizons. The evidence for an event is considered strong if multiple lines of evidence are observed in several trenches at precisely the same stratigraphic interval. Examples of phenomena used as evidence for past events are presented in Figs. 7, 8, 9 and 10. The electronic supplement includes a detailed event-by-event and exposure-by-exposure listing of pictorial evidence for each surface rupture from the various trenches at Hog Lake.

Evidence for surface faulting was found at 21 stratigraphic horizons, although some of the evidence was weak or limited to two or three exposures only (Electronic supplement Table S1). For instance, the event 1 surface rupture breaks through unit 50 into unit 40 and is seen in some but not all exposures. The rupture produced only minor vertical separation of strata and we initially attributed this to possible after-slip after event 2. However, the observations of minor displacement match the field descriptions of minor displacement at Hog Lake reported after the April 1918 earthquake (Rolfe and Strong 1918), that produced intensity VII to IX damage from Riverside to Terwilliger Valley south of Anza (Toppozada and Parke 1982; Salisbury *et al.* 2012). The presence of liquefaction evidence in trench T2 that involves strata deposited after the penultimate rupture (electronic supplement B1, Figs. SB4, SB5, and SB6) supports the interpretation that this is the 1918 earthquake, because the site is usually under water in April. Furthermore, Salisbury *et al.* (2012) attribute at least 20 km of rupture to the 1918 earthquake northwest of Hog Lake in their preferred model, with an average of 1.25 m of displacement measured for this rupture. Finally, post-event 2 sedimentation occurred before event 1, thus indicating they are indeed separated by some time. Consequently, we interpret event 1 as the surface rupture from the 1918 earthquake.

Evidence for events 2, 3, and 4 are seen in most or all exposures, with event 2 occurring between units 60 and 57, event 3 between units 100 and 90, and event 4 between units 144a and 140 (electronic supplement, part B, Figs. SB1–SB30). Event 2 was interpreted by Salisbury *et al.* (2012) as the surface rupture of the 22 November 1800 earthquake, on the basis of historical reports, measured slip distribution attributed to the most recent large south-central San Jacinto rupture, and from knowledge of the results from the Hog Lake study which place the timing of event 2 in the late eighteenth century to earliest nineteenth century, as discussed below. Another possible option is the July, 1769 earthquake reported by the Portola expedition (Toppozada *et al.* 1981), although that earthquake seems to have been too small (M_w 5–6; Ellsworth 1990). Events 3 and 4 are dated to the sixteenth and fourteenth centuries,

Journal : Small 24 | Dispatch : 28-10-2014 | Pages : 23
Article No. : 955 | □ LE | □ TYPESET
MS Code : PAAG-1383 | ☑ CP | ☑ DISK

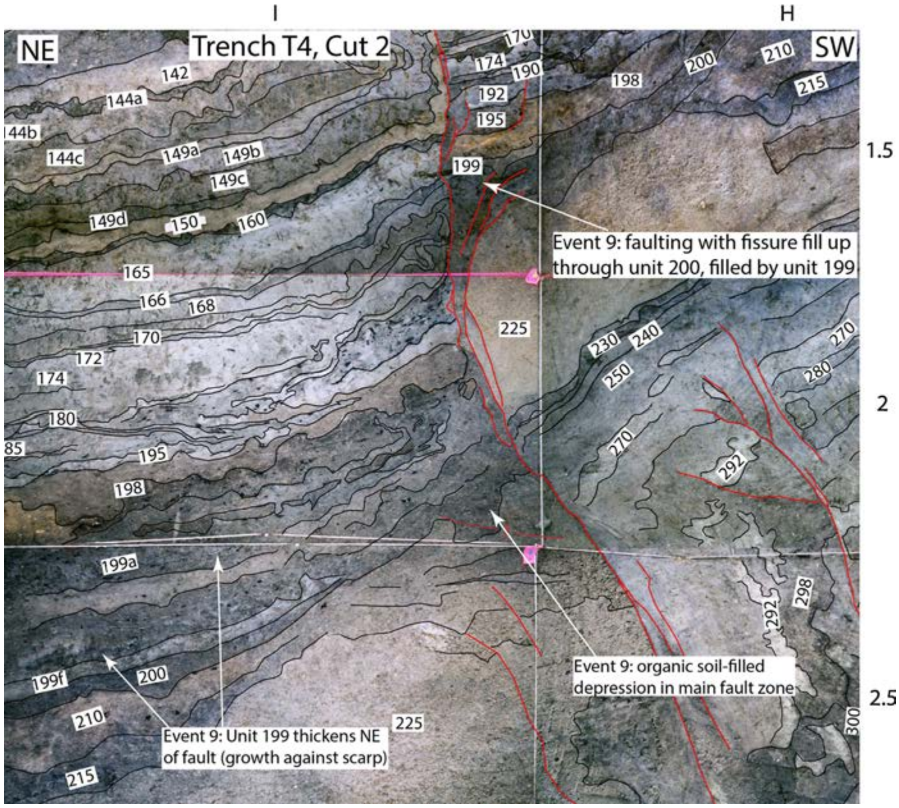

Figure 7
Example of a fissure filled with organic sediment that indicates a surface rupture between units 199 and 200 during event 9. Also note the growth strata on the down-thrown northeastern side of the fault. Gridding in this figure and in Figs. 8, 9, 10, and 12 is the same as on the full logs provided in the electronic supplement

respectively, and are clearly prehistoric in age (Fig. 10).

Events 5 and 6 occurred between units 144c/144b and between units 160/150, respectively. Of note is that these two events seem, on the basis of the radiocarbon dating, to have been closely spaced in time. Evidence was observed in some exposures only, suggesting that these may be smaller and more similar to event 1, or possibly intermediate in size.

The 21 event horizons and associated evidence are explicitly laid out in the electronic supplement (Figs. S2–S124), and the event ages are graphically shown in Fig. 11, in which both chronologic models are displayed. Of note is the observation that the ages of nearly all events remained stationary except for event 12, which was slightly younger in model 2. This observation indicates that the ages of the Hog Lake strata and interpreted event ages are robust.

The event evidence is summarized in Part B of Table S1 in the electronic supplement, in which each feature in each trench face is numerically rated from zero to three, with three being regarded as strong evidence. The rated features were divided into five categories: upward terminations; fissure fills; folding; angular unconformities; and presence of growth strata. Liquefaction features, where present, are noted in Figs. SB2–SB124, but are not used in the rating scheme because it is not always possible to determine where the ground surface was when liquefaction occurred. All of the evidence elucidated in one of the figures in the electronic supplement is assigned a value of 1, 2, or 3, depending on the strength of the evidence. We have not described all examples of lower quality event evidence, although for some weaker events the lower quality observations are predominant. Some criteria are linked, and

Journal : Small 24 | Dispatch : 28-10-2014 | Pages : 23
Article No. : 955 | ☐ LE | ☐ TYPESET
MS Code : PAAG-1383 | ✔ CP | ✔ DISK

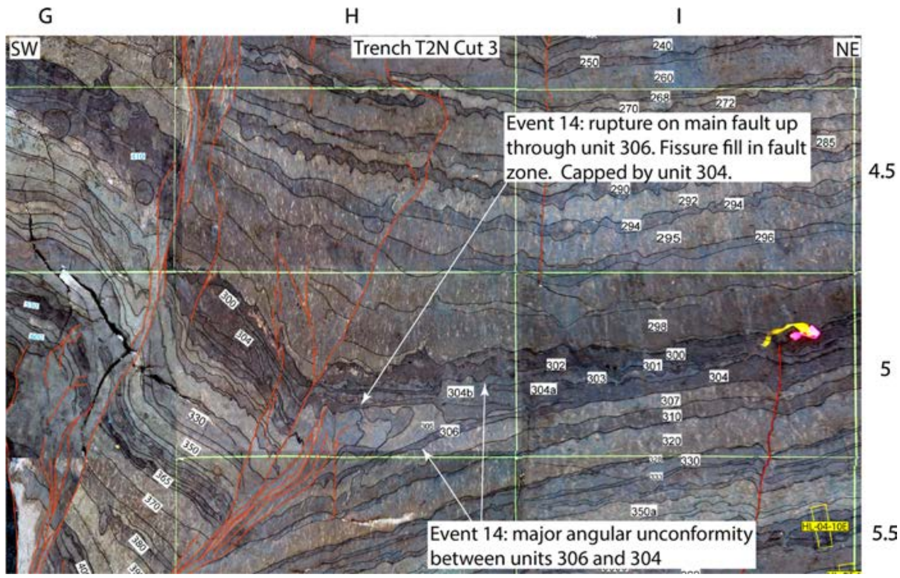

Figure 8
Example of an angular unconformity, upward terminations, and fissure fills associated with event 14, exposed in the north face of trench T2N, cut 3. A complete set of evidence for event 14 is given in the electronic supplement

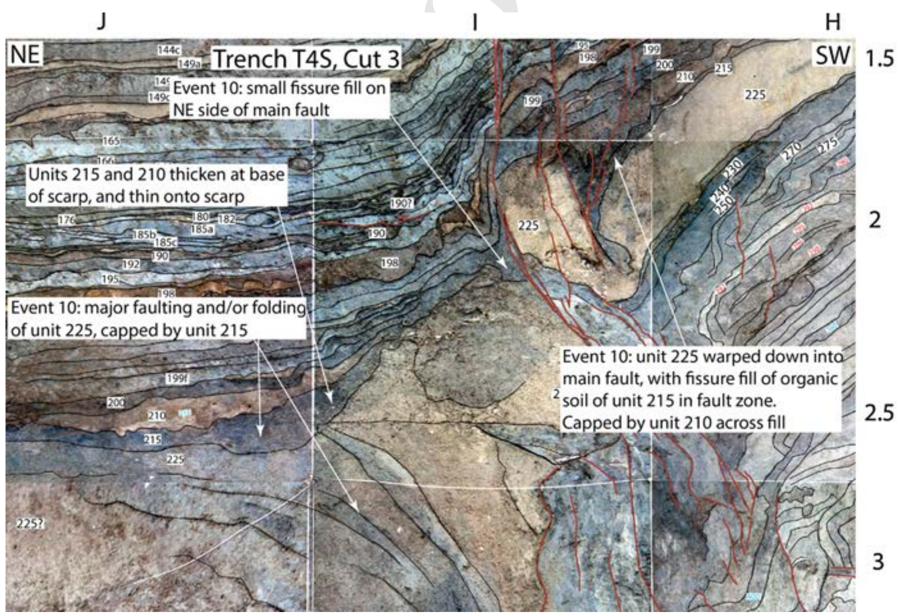

Figure 9
Example of a fissure fill, folding, upward termination, and growth section associated with event 10 in trench T4S, cut 3. Other evidence of event 10 is given in the electronic supplement

consequently may be double counted if both are present. For instance, folding is commonly associated with angular unconformities so both may be present in an exposure. Other exposures revealed angular unconformities but folding was not obvious. Similarly, filled fissures may also be upwardly terminated when capped by unbroken stratigraphy. Some weak evidence may be present in the images presented in the electronic supplement but were not considered sufficient to be worthy of description. In

Journal : Small 24 Dispatch : 28-10-2014 Pages : 23
Article No. : 955 □ LE □ TYPESET
MS Code : PAAG-1383 ✔ CP ✔ DISK

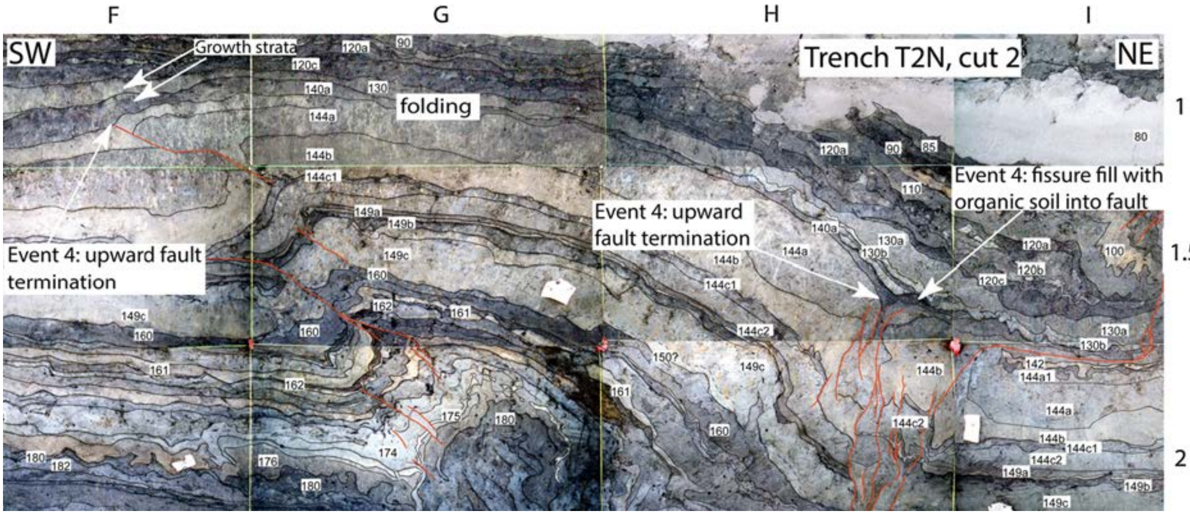

Figure 10
Example of folding with associated upward termination and growth strata on the secondary fault, and upward termination and fissure fill along main fault associated with event 4 in trench T2N, cut 2. Other evidence of event 4 is given in the electronic supplement

these cases, they were usually assigned 1 or possibly a 2, depending on our judgment. Without question, this exercise could be conducted by several people, yielding slightly different results, but overall should, if done consistently, provide a similar relative measure for rating the strength of each event.

Once each type of evidence was rated for each category, the ratings were summed for each interpreted event horizon and divided by the number of exposures that should have provided evidence for the event. If every exposure had every type of evidence and all were excellent (3), the score would be calculated as $5 \times 3 \times$ the number of trenches in which the evidence was present. For 10 trench exposures, this number could be as high 150. This value would then be divided by the number of trenches that exposed stratigraphy of the correct age, for a maximum weighted score of 15. As is common along strike-slip faults, no single exposure had all of the types of evidence, and some trench exposures were shallow and, consequently, record a shorter period of time and fewer events. Further, some trenches, for example Trench T1 had only limited or meager evidence because of being near the shoreline and having periods of non-deposition. Thus, the final scores range from 1.6 to 11.7. The historically reported 1918 earthquake, which produced only minor displacement at Hog Lake, rated the lowest score of 1.6. Other weak events ranged in score from 3 to 4.4, whereas many of the well-expressed interpreted events yielded scores in the 8–11 range. One interpretation is that the higher-scoring events were larger earthquakes, as we discuss below. Table 1 presents the event ages from model 2, the numeric scores from our rating scheme, and our interpretation of event size.

5.1. *Completeness of the Hog Lake Record*

The stratigraphy at Hog Lake is exceptional, with millimeter to centimeter resolution of the decimeter-scale strata. Nevertheless, at least two factors can lead to an incomplete record of surface ruptures at Hog Lake. First, re-rupture of the same fault strand in subsequent events can locally obliterate evidence of the earlier event, as is seen in some exposures with event 2 obscuring event 3 (Fig. 12). In such cases, our strategy has been to cut many exposures and demonstrate consistency of the event evidence from exposure to exposure. Although there is no definitive way of testing for completeness, the events with abundant evidence seem to also control sedimentation and the deposition of growth strata, separate indicators of an event, and we believe we have probably captured all of the largest events unless multiple earthquakes occurred during a period of non-deposition. However, smaller events similar to the 1918 rupture may not cause folding and angular unconformities, or force deposition of growth

Journal : Small 24 | Dispatch : 28-10-2014 | Pages : 23
Article No. : 955 | ☐ LE | ☐ TYPESET
MS Code : PAAG-1383 | ☑ CP | ☑ DISK

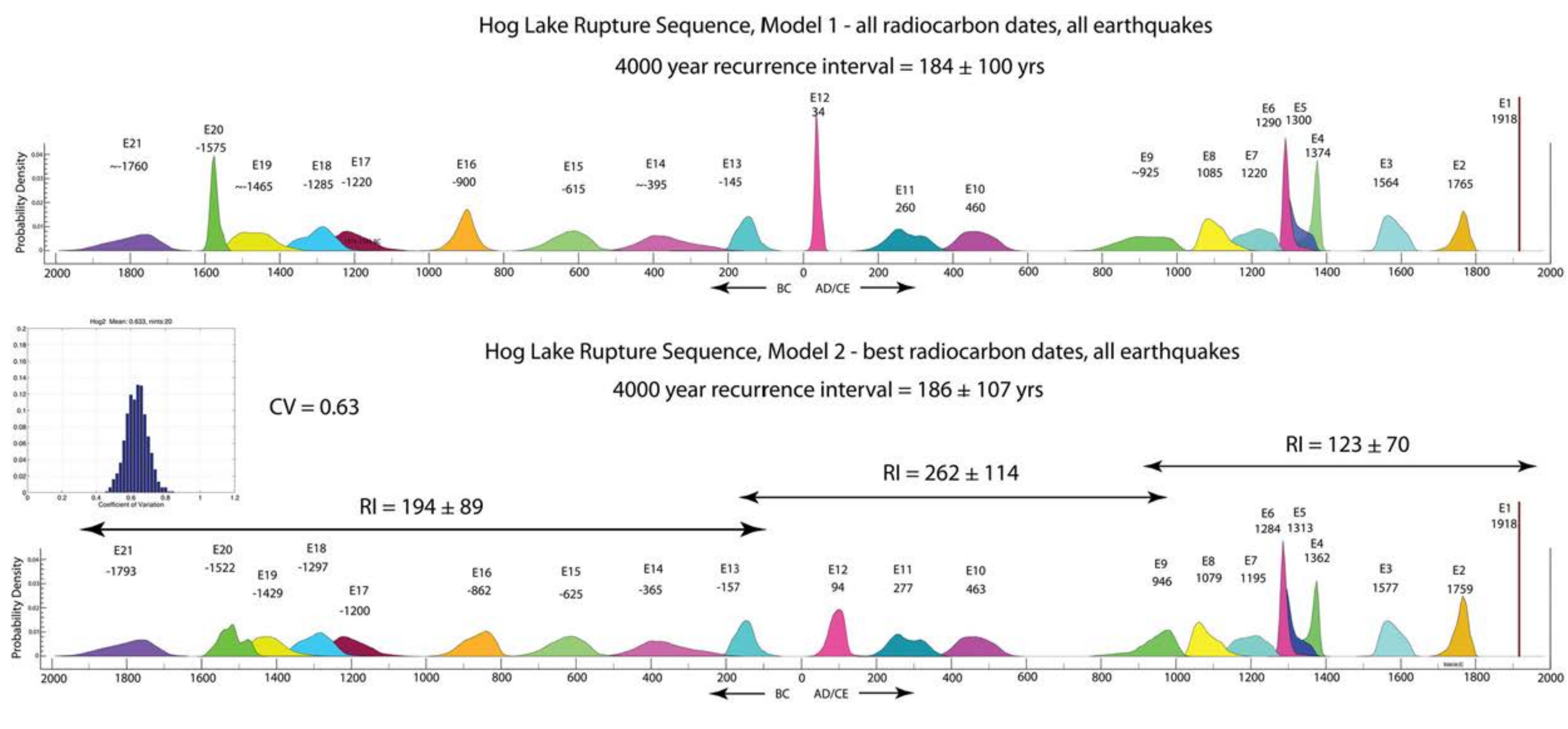

Figure 11
Model ages of surface ruptures identified at Hog Lake. Model 1 uses all 97 radiocarbon dates that do not violate stratigraphic ordering, although some dates mostly fall outside the age window expected, on the basis of overlying and underlying dates. Model 2 uses only the 85 dates that are well ordered in OxCal, and is our preferred model. Note that most of the model ages of events did not change much or at all

Journal : Small 24 | Dispatch : 28-10-2014 | Pages : 23
Article No. : 955 | ☐ LE | ☐ TYPESET
MS Code : PAAG-1383 | ☑ CP | ☑ DISK

strata, and if rupture recurs on the same fault strand, evidence for such small events may be completely obliterated. Consequently, we believe it possible that some 1918-type earthquakes may be present at Hog Lake, but for which we have no evidence.

Another possible reason all major events are not accounted for is if two ruptures occur during a drought or period of non-deposition, in which case they could appear as a single event. Although we have no evidence this has occurred, major accumulation of organics is apparent in units 198–200, and several oxidized layers suggest several episodes of burning of the marsh surface. This is likely to indicate that the rate of deposition was low during the time period which included events 9 and 10 and leaves open the possibility of a missed event, despite the many trench faces that expose this part of the section.

6. *Discussion*

Several observations and conclusions can be made from the long rupture record of Hog Lake. We first discuss the long-term pattern of earthquake recurrence, then discuss the likelihood of the next large earthquake. We compare the recurrence interval and information on slip per event (Salisbury *et al.* 2012) with the long-term slip rate (Blisniuk *et al.* 2013) to better understand the context in observed variations in earthquake production. We then compare the rupture history at Hog Lake with that at Mystic Lake (Onderdonk *et al.* 2013; personal communication) and at sites along the San Andreas Fault, both north and south of its juncture with the San Jacinto Fault, to develop plausible rupture scenarios for the past millennia or so, and to investigate possible modes of fault and segment interaction.

6.1. *Pattern of Occurrence and Recurrence Interval at Hog Lake*

To the eye, the pattern of occurrence of surface ruptures at Hog Lake is generally quasi-periodic in the long-term, although there was at least one cluster or "flurry" of four ruptures within a 150-year period between approximately AD 1200 and 1350 (Fig. 11). Of note, one of these ruptures, event 5, was given a relatively low score of 3.5, which may indicate that this earthquake was smaller than the full Clark fault rupture

Table 1

Mean event ages and age ranges, and interpreted relative size of earthquakes for the Hog Lake sequence

Earthquake events	Mean age AD/BC	Age range	Event score	Interpreted event size
E1	1918[a]		1.6	Moderate
E2	1761[b]	AD 1,723–1,797	8.1	Large
E3	1577	AD 1,535–1,627	9.7	Large
E4	1357	AD 1,303–1,389	10.2	Large
E5	1311	AD 1,280–1,362	3.5	Moderate
E6	1289	AD 1,267–1,315	5.5	Moderate or large
E7	1193	AD 1,118–1,267	8.6	Large
E8	1080	AD 1,028–1,144	4.4	Moderate
E9	947	AD 842–1,020	9.2	Large
E10	462	AD 382–545	11.7	Large
E11	280	AD 204–361	7.2	Large
E12	94	AD 51–130	5.6	Moderate or large
E13	−158	293–80 BC	8.8	Large
E14	−364	486–222 BC	7.8	Large
E15	−624	724–541 BC	3	Moderate
E16	−863	941–798 BC	7	Large
E17	−1208	1,303–1,104 BC	5.75	Moderate or large
E18	−1295	1,373–1,223 BC	3.7	Moderate
E19	−1434	1,532–1,340 BC	3	Moderate
E20	−1520	1,580–1,457 BC	7.5	Large
E21	−1794	1,916–1,691 BC	6.5	Large

[a] Historically known; surface rupture identified by Salisbury *et al.* (2012)

[b] Probably the historically known November 22, 1800 earthquake

Journal : Small 24 | Dispatch : 28-10-2014 | Pages : 23
Article No. : 955 | ☐ LE | ☐ TYPESET
MS Code : PAAG-1383 | ☑ CP | ☑ DISK

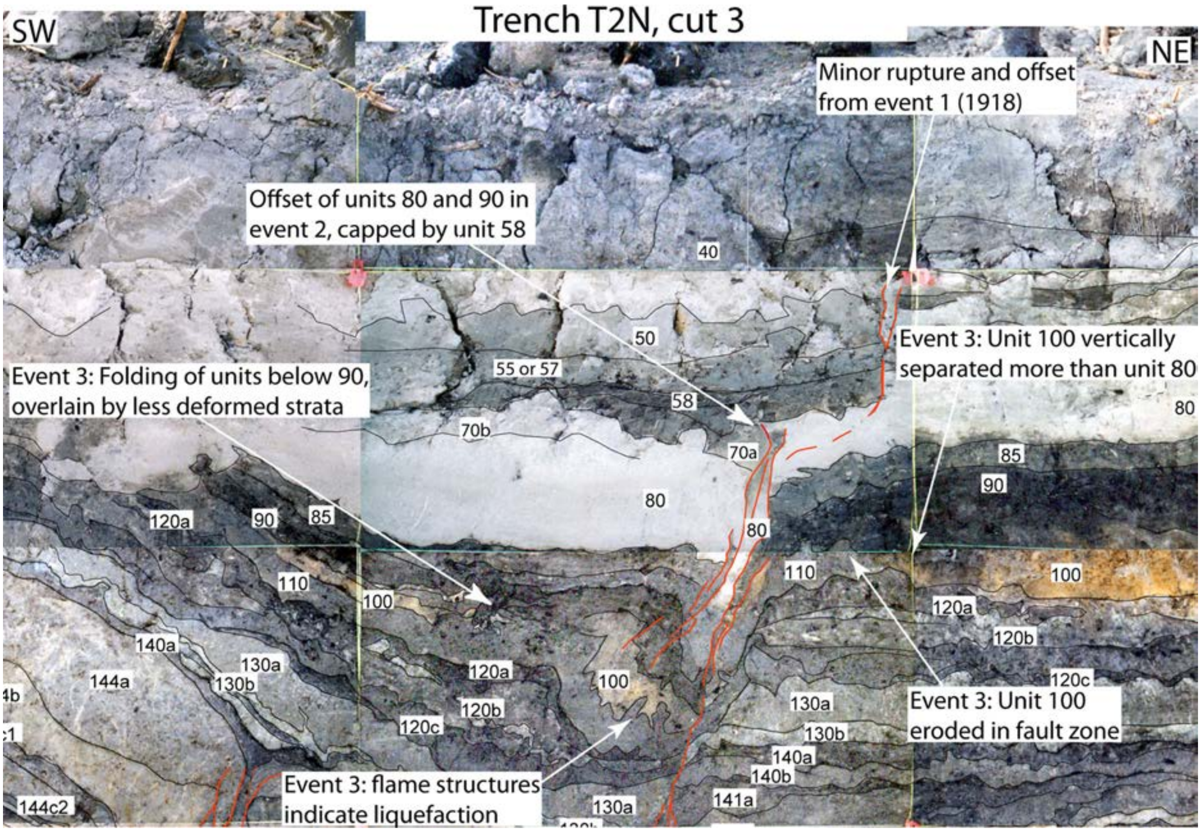

Figure 12
Re-rupture along the same narrow fault zone obscures evidence of earlier events. Here, event 3 caused displacement and folding of unit 100 down into the fault, capped by less deformed strata that are offset in event 2, and offset again, to a small extent, in event 1. Distinguishing events in which rupture has repeatedly occurred in the same location can be challenging

which we interpret as occurring in events 2, 3, and 4 on the basis of the work of Salisbury *et al.* (2012). Event 6 was given a moderate score of 5.5, which may indicate this, also, was a moderate event, although perhaps larger than event 5. Furthermore, events 5 and 6 have nearly identical ages, indicating that they probably occurred back-to-back, consistent with partial rupture of the Clark Fault, followed by a second shock. Alternatively, one or both of these events could be similar to the 1918 rupture but may have penetrated deeper into the Anza Seismic Gap than did the 1918 earthquake, explaining the better expression. We note, however, that the 1918 rupture (event 1) received the lowest score of any recognized event and that older such ruptures may have been completely obliterated by subsequent events. This may indicate that all of the recognized events before event 1 are larger than the 1918 earthquake, at least as recorded at Hog Lake.

The long-term recurrence interval was calculated by taking the peak probability of each event probability distribution (PDF) in model 2 and assigning a year to each event (Table 1). The intervals between each event were then used to determine the mean recurrence interval and its standard deviation. The coefficient of variation (COV) was calculated by dividing each event PDF into 10,000 pieces of equal probability and then using a random sampling approach to draw possible event histories for the site, requiring that the events be in chronologic order until 1,000 successful event histories have been achieved. The range of individual COVs for this sample of event histories is shown in Fig. 11.

Models 1 and 2 yielded similar recurrence intervals and standard deviations of 184 ± 100 and 186 ± 106 years, respectively (Fig. 11). The CoV of 0.63 was only calculated for model 2, our preferred

Journal : Small 24 Dispatch : 28-10-2014 Pages : 23
Article No. : 955 ☐ LE ☐ TYPESET
MS Code : PAAG-1383 ☑ CP ☑ DISK

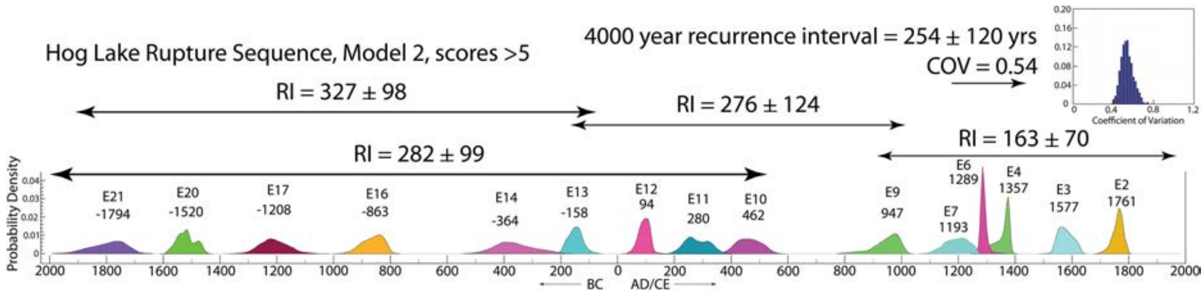

Figure 13
Plot of Hog Lake events with scores >5. This assumes that scores <5 represent rupture in smaller events. This model suggests a longer recurrence interval and more periodic ruptures between approximately 4 and 2.5 ka, and a shorter recurrence interval with more variability for the past 1–1.5 ka. Note that the interval sampled can yield factor of two differences in apparent recurrence intervals, arguing that short earthquake records are not reliable indicators of long-term recurrence

model that we carried forward. These values are for all recognized surface ruptures, including the weakly expressed ones. If we remove all inferred events with scores below 5 (Electronic Supplement, Part B, Table S1), assuming that scores below 5 represent smaller, 1918-type earthquakes that ruptured predominantly to the north, the recurrence interval lengthens to 254 ± 120 years with a CV of 0.54 (Fig. 13).

Another interesting aspect of this long record is that in some periods recurrence intervals have been longer or shorter than the long-term average. This is important, because most paleoseismic records are much shorter (a few events) and there is no way to determine if a short record is representative of the long-term average and it may, in fact, be quite misleading. For instance, considering all events, in the past millennium (events E1 through E9) the recurrence interval of 123 ± 70 years has been relatively short, owing to the flurry of events in the thirteenth to fourteenth century. In comparison, in the penultimate millennia (events 9 through 13) the recurrence interval of 262 ± 114 years was much longer, approximately twice as long as for events 1 through 9. Similarly, for the oldest two millennia (events 13 through 21) the recurrence interval was 194 ± 89 years, between that of the past two millennia (Fig. 13). These observations argue that recurrence intervals determined from short paleoseismic records may be in error by a factor of two, or more, when compared with those from a longer time sequence of events.

We calculated the likelihood of the next surface-rupturing event by taking all the identified ruptures, including 1918, and using the recurrence interval calculated from the chronology of method 2. Using a Brownian passage time (BPT) model (Ellsworth *et al.* 1999; Matthews *et al.* 2002), we calculated a conditional probability of 0.20 for a surface rupture in the next 30 years. If we discount the 1918 earthquake, which had minimum expression at Hog Lake, and assume the other 20 earthquakes are large, the conditional probability is slightly higher at 0.23. If we use the recurrence interval for the past millennia, 123 ± 70 years, and assume that this best represents the current pattern of strain release, the probability increases to 0.34. In contrast, if we only take the well-represented ruptures presented in Fig. 13 with a recurrence interval of 254 ± 120 years and a lapse time of 214 years, the probability of a repeat of the November 1800 earthquake in the next 30 years drops to 0.19. In all cases, the conditional probability of a large earthquake on the central San Jacinto Fault is close to 20 % in the next 30 years, irrespective of the model used. However, if a significant number of 1918-type earthquakes have ruptured at Hog Lake but been obscured in a complex manner by the larger events, the likelihood for a northern Clark rupture may be higher.

It is interesting to compare the average recurrence interval for full fault ruptures with the long-term slip rate of $12.1^{+3.4/-2.6}$ mm/year (Blisniuk *et al.* 2013) and the average displacement near Anza of 3–3.5 m as determined from the slip distributions of the last three Hemet to Clark Valley ruptures (Salisbury *et al.* 2012) and back-calculate the estimated rate of recurrence. Using this method, we calculate a return period for the larger ruptures to be $268^{+100/-75}$ years,

Journal : Small 24 | Dispatch : 28-10-2014 | Pages : 23
Article No. : 955 | ☐ LE | ☐ TYPESET
MS Code : PAAG-1383 | ☑ CP | ☑ DISK

similar to or slightly larger than the recurrence interval we determined if only observed ruptures with event scores >5 are used to estimate the recurrence of large ruptures. If we use only the 14 ruptures in the model where we removed the smaller events in the "flurry", and assume 3.25 m of slip per event (Salisbury *et al.* 2012), the predicted slip rate is about 12 mm/year, consistent with the long-term rate.

6.2. Comparison with Mystic Lake

The Clark strand enters the Hemet Valley where it is buried by young alluvium, but continues as the Casa Loma strand where scarps in the alluvium northwest of Hemet are expressed (Marliyani *et al.* 2013). The Claremont strand is separated from the Casa Loma strand at the "Hemet step-over" at Mystic Lake, a step-over distance of 2.25 km (Marliyani *et al.* 2013). Large earthquakes are capable of rupturing through a releasing step of this size (Wesnousky 2008), suggesting that the entire central and northern San Jacinto Fault could fail in a single large earthquake.

We plotted the most recent 12 event ages from Hog Lake (chronologic model 2) against the 11 event ages determined at Mystic Lake along the Claremont strand of the San Jacinto Fault for the same time period (Fig. 14) (Onderdonk *et al.* 2013, in preparation). Several of the event PDFs at Hog Lake match the event PDFs at Mystic Lake, enabling their possible correlation. In these cases, we cannot definitively state that these are the same events, because of broad age uncertainties, but this interpretation is plausible. In contrast, several events at Hog Lake do not have a match at Mystic Lake, and several at Mystic Lake have no possible correlation at Hog Lake. Hence, if the dates are reliable, at least half of the ruptures at Mystic and Hog Lake are not continuous between the two sites.

6.3. A Rupture Model for the Central and Northern San Jacinto Fault

We combined the paleoseismic data from Hog Lake and Mystic Lake with historical earthquake data and the limited information on slip distribution for the past several central San Jacinto events to construct a plausible rupture history of the central and northern San Jacinto Fault for the past 1.5 millennia (Fig. 15). In this model, we assume that the Claremont strand typically fails in large events that rupture the entire northern section of the fault, from Mystic Lake to its juncture with the San Andreas fault, and that the events observed at Mystic Lake represent such ruptures. We assume that we do not see smaller or moderate events, for example the 22 July 1899 Lytle Creek earthquake (plausibly as large as M6.5; Toppozada *et al.* 1981) or the 23 July 1923 Riverside earthquake (M6 according to Toppozada *et al.* 1981; we question whether this event occurred on the San Jacinto Fault). Similarly, we do not expect to see ruptures associated with 1937-sized earthquakes along the Clark Fault, in part because the magnitude was probably too small for surface rupture (~M6).

For the Clark strand, we assume that well-expressed events at Hog Lake represent ruptures that extend the full length of the Clark Fault, or may cascade on to segments to the north, and that weakly-expressed events are similar to the 1918 rupture. For 1918-type ruptures, we use Salisbury *et al.* (2012) and extend the ruptures from Hog Lake (or slightly south) to as far north as Park Hill in Hemet. We use Park Hill because it is a restraining step of moderate dimensions (1.5–2 km step) and the 1918 earthquake ruptured at least as far north as the mouth of Bautista Canyon with up to 50 cm of displacement (Salisbury *et al.* 2012). Hence, if displacement continued to drop off to the north in the subsurface, where the Hemet Valley deepens and there is thick alluvial cover, the rupture may have extended as far northwest as Park Hill, situated about 5 km northwest from the mouth of Bautista Canyon.

For the Casa Loma Fault, there are no paleoseismic data to constrain its past rupture history. For this model, we assume that the Casa Loma strand ruptures with the Clark and Claremont fault for events that are plausibly correlative at Mystic and Hog Lake, and we assume it ruptures independently in 1899-type events or with Hog Lake events for the balance of the moment release.

We use the relationship in Eq. 1 to estimate the average magnitude of earthquakes that rupture a fault section (Sommerville *et al.* 1999; Hanks and Bakun

Journal : Small 24 Dispatch : 28-10-2014 Pages : 23
Article No. : 955 LE TYPESET
MS Code : PAAG-1383 CP DISK

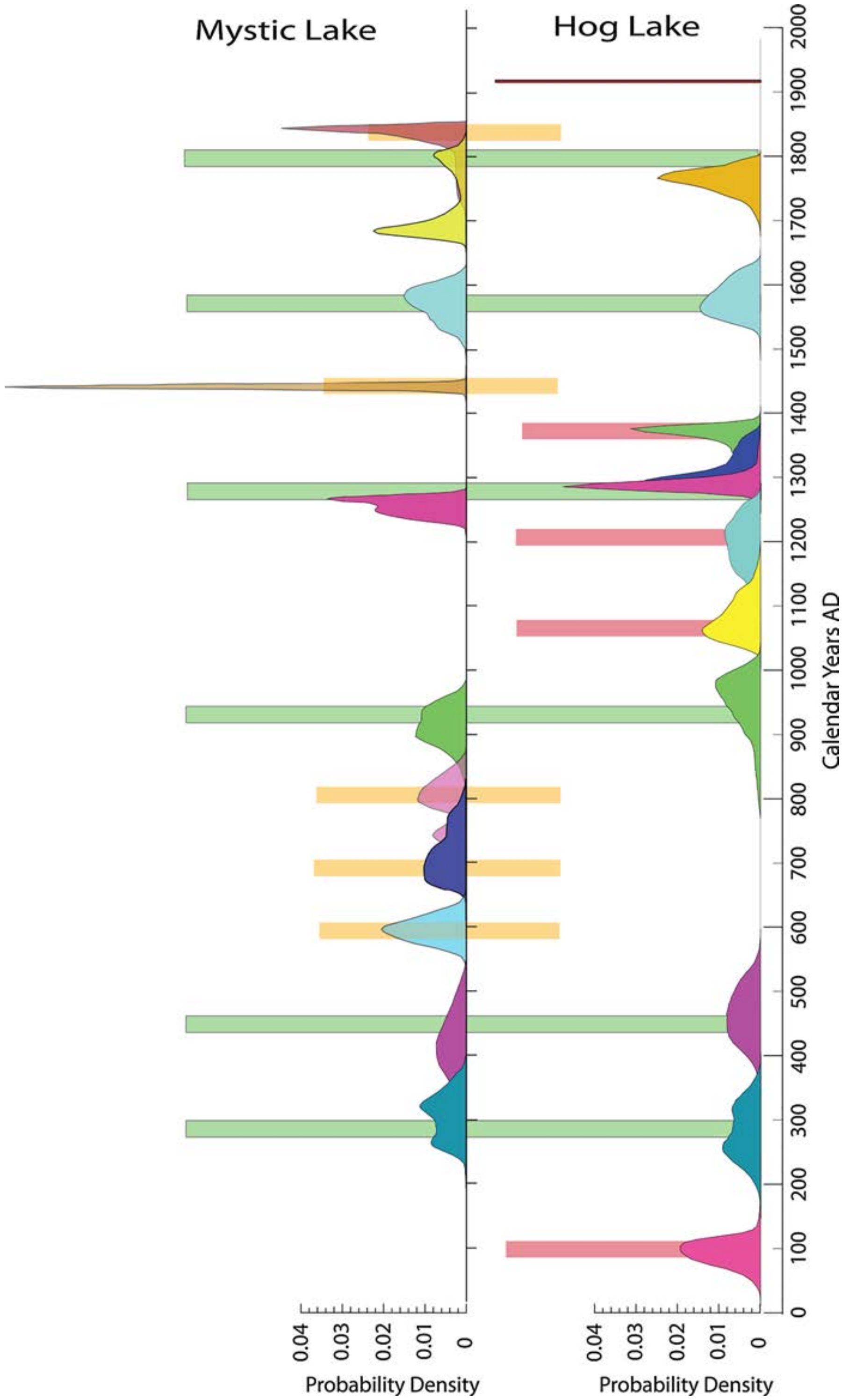

Figure 14
Comparison of the Hog Lake and Mystic Lake rupture records. *Green bars* indicate events that may correlate between the two sites, whereas *pink bars* indicate ruptures at Hog Lake that do not have a corollary at Mystic Lake and *yellow bars* indicate events at Mystic Lake that do not have a match at Hog Lake. From this plot, we argue that at least half of northern San Jacinto Fault ruptures do not jump the "Hemet" step-over at Mystic Lake

Journal : **Small 24**	Dispatch : **28-10-2014**	Pages : **23**
Article No. : **955**	☐ LE	☐ TYPESET
MS Code : **PAAG-1383**	☑ CP	☑ DISK

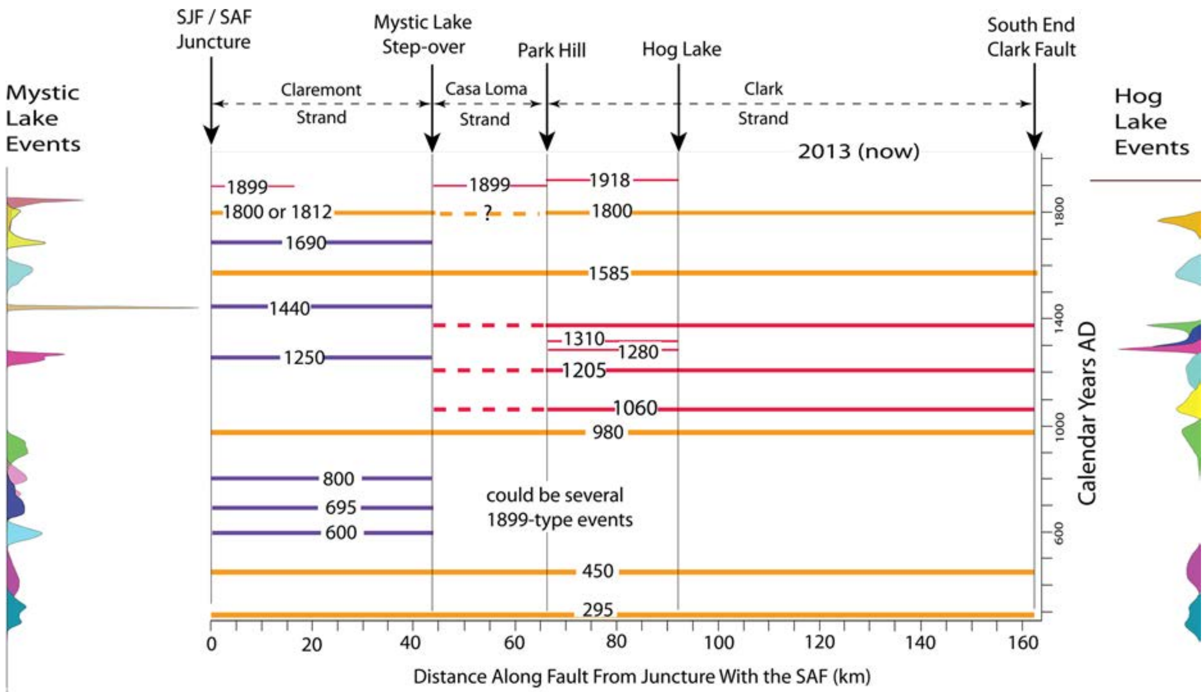

Figure 15
Rupture model for the Clark, Casa Loma, and Claremont strands of the San Jacinto Fault. Events in *red* are those identified at Hog Lake that do not have a possible correlation at Mystic Lake. Events in *orange* may correlate between Hog and Mystic Lakes, but might not. Events in *purple* are Mystic lake ruptures that do not have a possible correlation at Hog Lake. The locations of the historical earthquakes are inferred from their isoseismal areas and from mapping of the 1918 and 1800 ruptures (Salisbury *et al.* 2012). Summation of inferred moments yields a moment rate consistent with 12.2 mm/year of strain release for the past 1,700 years

2002, 2008). For rupture area, we take the segment length and use a seismogenic width of 15 km for the Casa Loma and Claremont faults, and 16 km for the Clark Fault. In fact, seismicity reaches as deep as 22 km near Anza (Sanders and Magistrale 1997), but shallows significantly toward the south, so the 16 km depth is an average value.

$$M_w = 3.98 + logA \qquad (1)$$

On the basis of Eq. 1, we calculated that rupture of individual fault segments can produce M_w of 6.8 for the Claremont Fault, 6.5 for the Casa Loma Fault, 6.7 for the northern Clark Fault from Park Hill to Hog Lake, and 7.2 for the entire Clark Fault. Alternatively, using the rupture distribution for the 1918 and 1800 earthquakes determined by use of offset geomorphic features (Salisbury *et al.* 2012), and the depth of seismicity along the Clark Fault (extends to as deep as 20 km in the Anza area, with 15–18 km depths to the NW and SE; Sanders and Magistrale 1997; Marliyani *et al.* 2013) to estimate fault width, we calculate the moments in these earthquakes to be approximately 1.5×10^{26} and 1.3×10^{27} dyne-cm, respectively, or moment magnitudes of 6.75 and 7.3, respectively, similar to the magnitude estimates based on rupture area. Estimating moment release for the Casa Loma Fault assuming 1 m of displacement [similar to 25 December 1899) and the Claremont Fault, assuming 2.25 m of displacement [based on the recurrence interval of 185 ± 25 years from Onderdonk *et al.* (2013)] and a 12–13 mm/year slip rate (Blisniuk *et al.* 2013) yields values of 1.1×10^{26} and 4.6×10^{26} dyne-cm, respectively, which equate to M_w 6.7 and 7.1 earthquakes, respectively.

Applying these estimates of moment for individual fault sections, and using the earthquake history presented in Fig. 15, we calculated a total moment release of approximately 1.7×10^{28} dyne-cm for the past 1,700 years, which yields a moment rate of 9.9×10^{24} dyne-cm/year. This moment rate is consistent with a fault slip rate of 12.2 mm/year, assuming 16 km for the average seismic depth. This

Journal : Small 24 Dispatch : 28-10-2014 Pages : 23
Article No. : 955 □ LE □ TYPESET
MS Code : PAAG-1383 ✔ CP ✔ DISK

inferred rate is within the range of the long-term rate determined at Anza (Blisniuk *et al.* 2013) and argues that the past 1,700 years has experienced a sufficient number of earthquakes along the San Jacinto fault to accommodate its long-term slip rate. These data also suggest there is no need to consider rare very large magnitude earthquakes, as applied in the UCERF3 models to account for underprediction of total slip.

Onderdonk *et al.* (2013) suggest that some northern San Jacinto earthquakes may coincide with earthquakes documented on the San Andreas Fault at Wrightwood. For instance, event E1 at Mystic Lake could match the timing of either the 12 December 1812 earthquake on the San Andreas Fault (Fumal *et al.* 2002) or event 2 at Hog Lake, which we infer was the 22 November 1800 earthquake. The 1800 earthquake is only reported from San Juan Capistrano and San Diego, both with MMI VII damage (Toppozada *et al.* 1981), which supports rupture of the central to southern San Jacinto Fault but not to the north. The 1812 earthquake was reported from San Diego and San Luis Rey (MMI V), San Juan Capistrano (MMI VII, but this intensity is based on collapse of the mission towers that were previously damaged in the 1800 earthquake; no adobes were damaged), San Gabriel (MMI VII), San Fernando (MMI VII), San Bernardino (MMI VI+), and San BuenaVentura (MMI VII?) and clearly had a more northerly source than 1800. However, if the 1800 earthquake had ruptured as far north as the Claremont strand, it is rather surprising that none of the northern missions reported damage from this earthquake. It is more likely the 1800 earthquake was limited to the Clark fault, which is also supported by the observations of displacement (Salisbury *et al.* 2012) that indicate that slip decreases toward the Hemet area.

In Fig. 16, we plot the event ages from Hog Lake and Mystic Lake and compare them with the event ages documented for Wrightwood (Fumal *et al.* 2002), Pitman Canyon (Seitz *et al.* 2000), and Burro Flats (UCERF 2 and 3). For ruptures that involve both the northern San Jacinto and the San Andreas Faults north of the common juncture, we expect to not observe evidence for an event at Pitman Canyon or Burro Flats, which are located southeast of the juncture.

Taken at face value, event 1 at Mystic Lake matches well the timing of the 1812 earthquake, but evidence for 1812 has also been reported from both Pitman Canyon and Burro Flats. This observation calls into question whether Mystic event 1 could be associated with the 1812 earthquake unless both faults ruptured nearly simultaneously as two discrete shocks. In contrast, a Wrightwood event in ca 1,700 could correspond to Mystic Lake event 2, and does not match well with event 2 from Pitman Canyon. Two older events at Mystic Lake match the timing of events at Wrightwood, although the Pitman Canyon record does not extend that far back in time to provide a test. In summary, up to four events recognized at Mystic Lake may have corresponding events at Wrightwood, although event correlations cannot be proved because of the uncertainties in event ages. In contrast, none of these four events have possible matches to events at Hog Lake, so if the northern San Jacinto occasionally does rupture with the San Andreas, it seems the south-central San Jacinto is not involved in the same events.

6.4. *Mode-Switching*

Finally, a comment on mode-switching as an explanation of the observed behavior of the Clark Strand of the San Jacinto Fault. Mode-switching is a self-driven switching back and forth between two modes of activity during steady tectonic loading which can result in clusters of earthquakes alternating with periods of lower seismic activity (Ben-Zion *et al.* 1999). The long record of earthquakes documented at Hog Lake indicates that for much of the past 4,000 years the fault ruptured in a quasi-periodic fashion. In the past 1,000 years, in contrast, a flurry or cluster of four earthquakes occurred in a 150-year period, and the overall recurrence interval is much shorter. As described above, this may be explained if some of the observed ruptures are 1918-type events that caused only minor rupture at Hog Lake. Event 6, however, had a moderately high score (Table 1), and even the events with scores above 3.5 are significantly better expressed than the 1918 earthquake, so all could have been larger earthquakes. If so, mode-switching may be an explanation of why the fault

Journal : Small 24 | Dispatch : 28-10-2014 | Pages : 23
Article No. : 955 | LE | TYPESET
MS Code : PAAG-1383 | CP | DISK

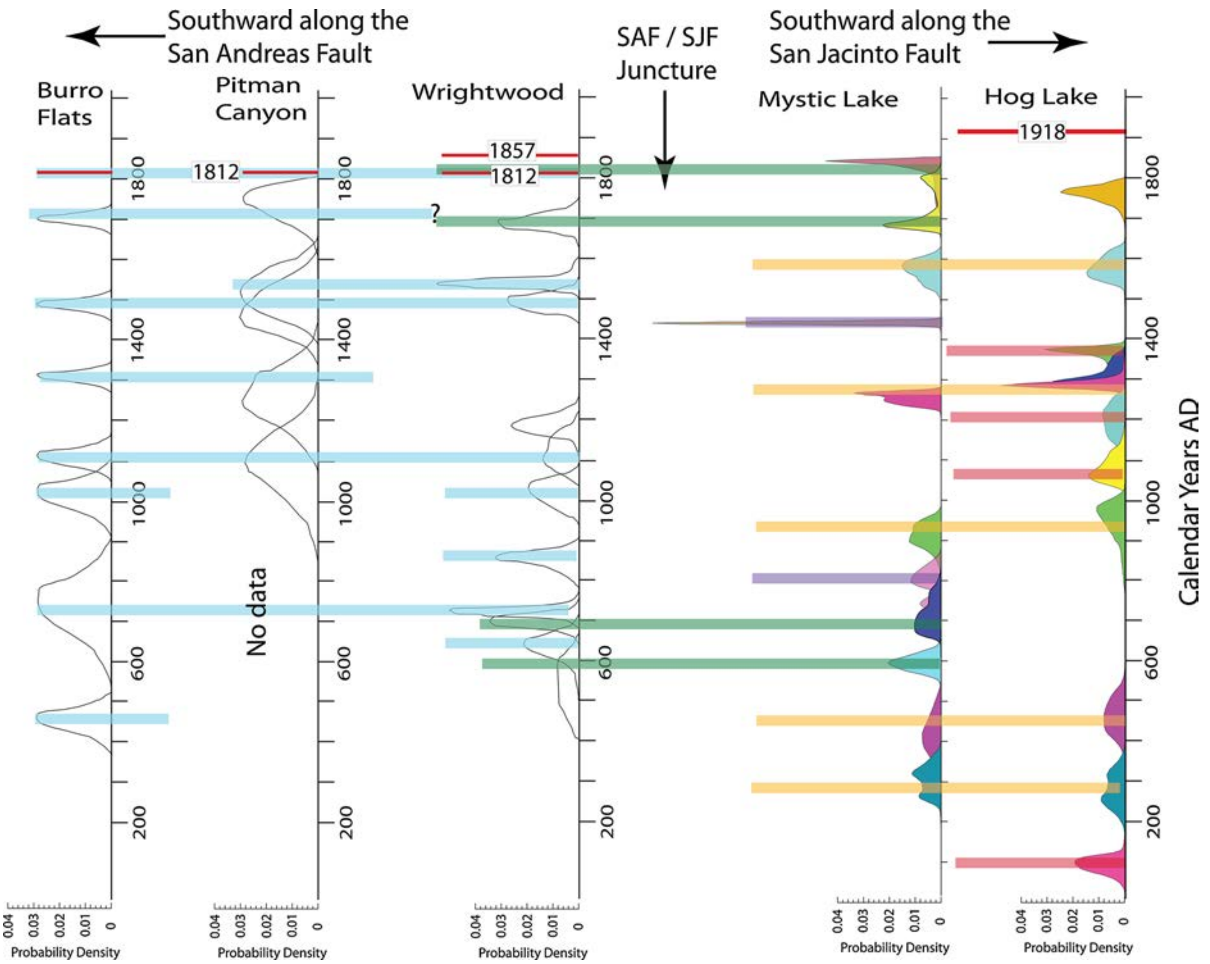

Figure 16
Plausible rupture scenarios involving the San Andreas and San Jacinto faults. As for Fig. 15, *red bars* indicate Hog Lake ruptures that do not correlate with Mystic Lake events, and *purple bars* are Mystic Lake events that do not have possible correlations with Hog Lake or Wrightwood. The *orange bars* indicate events that may correlate between Hog Lake and Mystic Lake, whereas *green bars* are possible matches between Mystic Lake and Wrightwood. The *blue bars* seem to be strictly San Andreas Fault events. Note that none of the possible Mystic-Wrightwood events seems to have ruptured as far south as Hog Lake, and that none of the possible Hog-Mystic Lake matches are observed at Wrightwood

experienced a spate of earthquakes, switching between quasi-periodicity and clustered behavior. It is interesting to note that the cluster of earthquakes at Hog Lake corresponds to a relative dearth of events on the San Andreas fault at Wrightwood. Similarly, the sparseness of Hog Lake events between about AD 500 and 900 corresponds to a "flurry" of events at Wrightwood (Fumal *et al.* 2002). As the Claremont strand experienced repeated rupture in this time period, and relatively few events during the Hog Lake "flurry", it is unlikely that the San Andreas and San Jacinto faults simply traded off in accommodating plate margin slip in these periods. Irrespective of the explanation of the cluster of earthquakes at Hog Lake, the fault has apparently switched back to quasi-periodicity, at least for the past several large events, suggesting that longer recurrence intervals may apply for a repeat of the 1800 earthquake.

7. Conclusions

Fault behavior is governed by a multitude of variables, for example fault complexity and rock

Journal : Small 24 | Dispatch : 28-10-2014 | Pages : 23
Article No. : 955 | ☐ LE | ☐ TYPESET
MS Code : PAAG-1383 | ☑ CP | ☑ DISK

heterogeneity, changes in stress from previous ruptures, and ruptures and stresses along regional faults. Seismic gaps, for example the Anza seismic gap, are of particular interest because they may shed light on fault behavior, for example the periodicity of large ruptures. This in turn could be used in earthquake forecasting.

The long, continuous record at Hog Lake reveals the behavior of the San Jacinto Fault for much of the past 4,000 years and indicates that the fault in this area typically ruptures in quasi-periodic large events. We also recognize the occurrence of smaller events, for example that which occurred in 1918, which are inferred to represent ruptures to the north between the Anza seismic gap and Hemet. The recurrence interval has varied by a factor of two over the past 4 ka, when sampled in 1-ka intervals; this observation suggests that short paleoseismic records may provide misleading indicators of long-term recurrence and earthquake production on major faults.

Comparison of the Hog Lake earthquake record with other records along the same fault and along the San Andreas Fault suggests that rupture of the entire south-central and northern San Jacinto Fault is possible but rare. The northern San Jacinto Fault may fall with the San Andreas Fault north of their common juncture, but if the San Andreas and full San Jacinto Faults have ruptured together, it would have been before the 2,000 years-long Mystic Lake record, and expression of the faulting at Hog Lake would have had to have been similar in magnitude to that for the historic AD 1800 event.

The average recurrence interval on the south-central San Jacinto Fault has varied over the past 4,000 years, with a long-term average of approximately 185 ± 100 years, irrespective of the chronologic model used. The recurrence interval for the past millennium has been much shorter at 123 ± 70 years, possibly because of better recognition of 1918-type ruptures or possibly because of mode-switching between quasi-periodicity and clustering. If weakly expressed events become smaller, 1918-type ruptures that only involve the northern part of the Clark strand, then the recurrence interval for larger earthquakes lengthens to 254 ± 120 years, and they have quasi-periodic behavior with a coefficient of variance of 0.54. The 30-year probabilities vary from approximately 0.19 to 0.22, depending on which choice of events and on which timeframe is assumed, but suggests that the likelihood of a large earthquake on the south-central San Jacinto fault is less than that expected for the southernmost San Andreas fault, which has been largely dormant for 300 years (Sieh and Williams 1990). In any case, when the south-central San Jacinto Fault does rupture in the future, it is likely to be in the M_w 7.3 range if limited to the Clark Fault, or larger if it also involves the Casa Loma and Claremont Faults.

Acknowledgments

We sincerely thank Manuel and Joe Hamilton for access to Hog Lake and the Ramona Indian Reservation. We also thank the many students and colleagues that joined us for a day or week for field assistance or review, including (but not limited to) Ramon Arrowsmith and his balloon team, Aron Meltzner, Danielle Verdugo, Daniel Ragona, Heitero Kaneda, Tom Fumal, and Dave Schwartz. Finally, we thank Kate Scharer and Glenn Biasi for providing excellent and detailed reviews that led to substantial improvement in the presentation and application of statistics. This research was supported by the National Science Foundation award EAR-0908515, the US Geological Survey NEHRP program grants 04HQGR0083 and 08HQGR0063, and the Southern California Earthquake Center. SCEC is funded by NSF Cooperative Agreement EAR-1033462 and USGS Cooperative Agreement G12AC20038. The SCEC contribution number for this paper is 1936.

References

Barnes, P.M., H. C. Bostock, H. L. Neil, L. J. Strachan, and M. Gosling (2013). *A 2300-Year Paleoearthquake Record of the Southern Alpine Fault and Fiordland Subduction Zone, New Zealand, Based on Stacked Turbidites.* Bulletin of the Seismological Society of America, *103*, 2424–2446. doi:10.1785/0120120314.

Bennett, R.A., A.M. Friedrich, and K.P. Furlong (2004). *Co-dependent histories of the San Andreas and San Jacinto fault zones from inversion of geologic displacement rate data*, Geology, *32,* 961–964.

Journal : Small 24 | Dispatch : 28-10-2014 | Pages : 23
Article No. : 955 | ☐ LE | ☐ TYPESET
MS Code : PAAG-1383 | ☑ CP | ☑ DISK

Berryman, K., A. Cooper, R. Norris, P. Villamor, R. Sutherland, T. Wright, E. Schermer, R. Langridge, and G. Biasi (2012). *Late Holocene Rupture History of the Alpine Fault in South Westland, New Zealand*. Bull. Seismo. Soc. Am., *102*, 620–638. doi:10.1785/0120110177.

Ben-Zion, Y., K. Dahmen, V. Lyakhovsky, D. Ertas, and A. Agnon (1999). *Self-Driven Mode Switching of Earthquake Activity on a Fault System*, Earth Planet. Sci. Lett., *172/1–2*, 11–21.

Blisniuk, K., Rockwell, T., Owen, L, Oskin, M., Lippincott, C., Caffee, M., and Dorch, J. (2010). *Late Quaternary slip-rate gradient defined using high-resolution topography and 10Be dating of offset landforms on the southern San Jacinto fault, California*, J. Geophys. Res. Solid Earth, *115*, B08401.

Blisniuk, K., M. Oskin, A.-S. Mériaux, T. Rockwell, R. C. Finkel, and F. J. Ryerson (2013). *Stable, rapid rate of slip since inception of the San Jacinto fault, California*, Geophys. Res. Lett., *40*, 4209–4213. doi:10.1002/grl.50819.

Bronk Ramsey, C., Staff, R.A., Bryant, C.L., Brock, F., Kitagawa, H., der Plicht, J., Schlolaut, G., Marshall, M.H. (2012). *A complete terrestrial radiocarbon record for 11.2 to 52.8 kyr B.P.*, Science *338* (6105): 370–374.

Fialko, Y. (2006). *Inter-seismic strain accumulation and the earthquake potential on the southern San Andreas fault system*, Nature, *441*, 968–971.

Ellsworth, W.L. (1990). Earthquake history, 1769–1989. In The San Andreas Fault System, California, U.S. Geological Survey Professional Paper 1515, (6) 24 p.

Ellsworth, W.L., M.V Matthews, R.M. Nadeau, S.P. Nishenko, P.A. Reasenberg, and R.W. Simpson (1999). A physically-based earthquake recurrence model for estimation of long-term earthquake probabilities. In Earthquake Recurrence: State of the Art and Directions for the Future Workshop, Instituto Nazionale de Geofisica, Rome, 22–25 February, 1999.

Fumal, T. E., R. J. I. Weldon, G. P. Biasi, T. Dawson, G. G. Seitz, W. T. Fronst, and D. P. Schwartz (2002). *Evidence for large earthquakes on the San Andreas fault at Wrightwood, California, paleoseismic site: 500 to present*, Bull. Seismol. Soc. Am. *92*, 2726–2760.

Grant, L. B., and K. E. Sieh (1994). *Paleoseismic evidence of clustered earthquakes on the San Andreas fault in the Carrizo Plain, California*, J. Geophys. Res. *99*, 6819–6841.

Hanks, T. C., and W. H. Bakun (2002). *A blinear source-scaling model for M-log A observations of continental earthquakes*, Bull. Seismol. Soc. Am. *92*, 1841.

Hanks, T. C., and W. H. Bakun (2008). *M-log A observations of recent large earthquakes*, Bull. Seismol. Soc. Am. *98*, 490.

Lienkaemper, J. J., and P. L. Williams (2007). *A record of large earthquakes on the southern Hayward fault for the past 1800 years*, Bull. Seismol. Soc. Am. *97*, 1803–1819.

Lienkaemper, J.J., J. N. Baldwin, R. Turner, R. R. Sickler, and J. Brown (2010). *A Record of Large Earthquakes during the Past Two Millennia on the Southern Green Valley Fault, California*, Bulletin of the Seismological Society of America *103*, 2386–2403. doi:10.1785/0120120198.

Lin, G., Shearer, P., and Hauksson, E. (2007). *Applying a three-dimensional velocity model, waveform cross-correlation, and cluster analysis to locate southern California seismicity form 1981 to 2005*, J. Geophys. Res., *112*, B12309.

Lindvall, S. C., T. K. Rockwell, T. E. Dawson, J. G. Helms, and K.W. Bowman (2002). *Evidence for two ruptures in the past 500 years on the San Andreas fault at Frazier Mountain, California*, Bull. Seismol. Soc. Am. *92*, 2689–2703.

Marliyani, G.I., Rockwell, T. K., Onderdonk, N. W., and McGill, S. F. (2013). *Straightening of the northern San Jacinto Fault, California as seen in the fault-structure evolution of the San Jacinto Valley step-over*. Bull. Seismo. Soc. Am., *103*(1), 519–541.

Matthews, M.V., W. L. Ellsworth, and P. A. Reasenberg (2002). *A Brownian Model for Recurrent Earthquakes.* Bull. Seismo. Soc. Am, *92*, 2233–2250. doi:10.1785/0120010267.

McCalpin, J. G., T.K. Rockwell, and R.J. Weldon II (2009). *Paleoseismology of strike-slip tectonic environments*. International Geophysics Series, *95*, 421–496. doi:10.1016/s0074-6142(09)95006-9.

Merifield, P.M., Rockwell, T.K., and Loughman, C.C. (1991). A slip rate based on trenching studies, San Jacinto fault zone near Anza, California: *Engineering Geology and Geotechnical Engineering*, no. 27 (James McCalpin, ed.), pp. 28-1–28-21.

Onderdonk, N. W., Rockwell, T.K., McGill, S. F., and G. I. Marliyani (2013). *Evidence for seven surface ruptures in the past 1600 years on the Claremont fault at Mystic Lake, Northern San Jacinto fault zone*, California, Bull of Seismol. Soc. Am., *103*, 519–541.

Rockwell, T. K., C. C. Loughman, and P. M. Merifield (1990). *Late Quaternary rate of slip along the San Jacinto fault zone near Anza, Southern California*, J. Geophys. Res. *95*(6), 8593–8605.

Rolfe F. and A. M. Strong (1918). *The earthquake of April 21, 1918, in the San Jacinto Mountains*. Bull. Seismo. Soc. Am, *8*, 63–67.

Salisbury, J. B., T. K. Rockwell, T. J. Middleton, and K. W. Hudnut (2012). *LiDAR and field observations of slip distribution for the most recent surface ruptures along the central San Jacinto fault,* Bull. Seismol. Soc. Am. *102*, 598–619.

Sanders, C. O. and Kanamori, H. (1984). *A seismo-tectonic analysis of the Anza Seismic Gap, San Jacinto Fault Zone, Southern California*, J. of Geophys. Res, *89*(B7): 5873–5890.

Sanders, C. and H. Magistrale (1997). *Segmentation of the northern San Jacinto fault zone, southern California*. J. Geophys. Res. *102*, B12, 27,453–27,467.

Scharer, K.M., Weldon, R.J., Fumal, T.E., and Biasi, G.P. (2007). *Paleoearthquakes on the southern San Andreas fault, Wrightwood, CA 3000 to 1500 B.C.: A new method for evaluating paleoseismic evidence and earthquake horizons*: Bull. Seismo. Soc. Am, *97*, 1054–1093. doi:10.1785/0120060137.

Scharer, K.M., Biasi, G. P., Weldon, R. J. II, Fumal, T. E. (2010). *Quasi-periodic recurrence of large earthquakes on the southern San Andreas fault,* Geology. *38*, 555–558.

Seitz, G., Biasi, G.P., and Weldon, R.W. (2000). An improved paleoseismic record of the San Andreas fault at Pitman Canyon, *in* Noller, J.S., *et al.*, eds., Quaternary geochronology: Methods and applications: American *Geophysical Union Reference Shelf 4*, pp. 563–566.

Sharp, R. (1967). *The San Jacinto fault zone in the Peninsular Ranges of southern California*. Bull. Seismo. Soc. Am *78*, 705–730.

Sieh, K. E. (1978). *Prehistoric large earthquakes produced by slip on the San Andreas fault at Pallett Creek, California*, J, Geophys. Res. *83*, 3907–3939.

Sieh, K. and P. Williams (1990). *Behavior of the southermost San Andreas fault during the past 300 years*, J. Geophys. Res. *95*, 6629–6645.

Journal : Small 24 Dispatch : 28-10-2014 Pages : 23
Article No. : 955 ☐ LE ☐ TYPESET
MS Code : PAAG-1383 ☑ CP ☑ DISK

Stone, E., L. B. Grant, and J R. Arrowsmith (2002). *Recent rupture history of the San Andreas fault southeast of Cholame in the northern Carrizo Plain, California*, Bull. Seismol. Soc. Am. *92*, 983–997.

Sommerville, P, Irikura, K, Graves, R, Sawada, S, Wald, D, Abrahamson, N, Iwasaki, Y, Kagawa, T, Smith, N, and Kowada, A. (1999). *Characterizing crustal earthquake slip models for the prediction of strong ground motion*. Seism. Res. Lett. *70*, 59–80.

Toppozada, T.R., Real and D.L. Parke (1981). Preparation of isoseismal maps and summaries of reported effects for pre-1900 California earthquakes. California Div. Mines and Geology, Open File Report 81–11 SAC. 182 p.

Toppozada, T. R. and D. L. Parke (1982). Areas damaged by California earthquakes, 1900–1949, Calif. Div. Mines Geol. Open-File Rept. 82–17, 65 pp.

U.S. Geological Survey and California Geological Survey (2006). Quaternary fault and fold database for the United States, accessed July 16, 2013. http://earthquake.usgs.gov/hazards/qfaults/.

Weldon, R.J., McCalpin, J.P., and Rockwell, T.K. (1996). Paleoseismology in strike-slip tectonic environments: *Paleoseismology* (J. McCalpin, ed), Academic Press, San Diego, pp. 271–330.

Wesnousky, S. G. (2008). *Displacement and geometrical characteristics of earthquake surface ruptures: Issues and implications for seismic hazard analysis and the earthquake rupture process*, Bull. Seismo. Soc. Am, *98, 4*, 1609–1632.

Working Group on California Earthquake Probabilities and the California Earthquake Authority (2013). Uniform California Earthquake Rupture Forecast v. 3.

Young, J. J., J R. Arrowsmith, L. Colini, L. B. Grant, and B. Gootee (2002). *Three-dimensional excavation and recent rupture history along the Cholame segment of the San Andreas fault*, Bull. Seismo. Soc. Am. *92*, 2670–2688.

(Received October 31, 2013, revised July 22, 2014, accepted July 23, 2014)

Journal : Small 24 | Dispatch : 28-10-2014 | Pages : 23
Article No. : 955 | ☐ LE | ☐ TYPESET
MS Code : PAAG-1383 | ☑ CP | ☑ DISK